Charge transfer efficiency in a p-channel CCD irradiated cryogenically and the impact of room temperature annealing

Conference or Workshop Item

Charge Transfer Efficiency in a p-channel CCD irradiated cryogenically and the impact of room temperature annealing

J. P. D. Gow[a], N. J. Murray[a,b], D. Wood[a], D. Burt[c], D. J. Hall[a], B. Dryer[a] and A. D. Holland[a]
[a]Centre for Electronic Imaging, The Open University, DPS, Milton Keynes, MK7 6AA, UK
[b]Dynamic Imaging Analytics Ltd, Bletchley Park Science and Innovation Centre, Milton Keynes, MK3 6EB, UK
[c]e2v technologies plc, 106 Waterhouse Lane, Chelmsford, Essex, CM1 2QU, UK

ABSTRACT

It is important to understand the impact of the space radiation environment on detector performance, thereby ensuring that the optimal operating conditions are selected for use in flight. The best way to achieve this is by irradiating the device using appropriate mission operating conditions, *i.e.* holding the device at mission operating temperature with the device powered and clocking. This paper describes the Charge Transfer Efficiency (CTE) measurements made using an e2v technologies p-channel CCD204 irradiated using protons to the 10 MeV equivalent fluence of 1.24×10^{9} protons.cm^{-2} at 153 K. The device was held at 153 K for a period of 7 days after the irradiation before being allowed up to room temperature where it was held at rest, *i.e.* unbiased, for twenty six hours to anneal before being cooled back to 153 K for further testing, this was followed by a further one week and three weeks of room temperature annealing each separated by further testing. A comparison to results from a previous room temperature irradiation of an n-channel CCD204 is made using assumptions of a factor of two worse CTE when irradiated under cryogenic conditions which indicate that p-channel CCDs offer improved tolerance to radiation damage when irradiated under cryogenic conditions.

Keywords: CCD, p-channel, cryogenic irradiation, charge transfer efficiency, proton radiation damage

1. INTRODUCTION

The ionising and non-ionising damage caused by the space radiation environment, and secondaries from the spacecraft, has a negative impact on the performance of electronic systems. In the case of optoelectronic devices the loss in performance is primarily caused by incident protons which can form defects within the silicon bandgap. Lattice defects change the electrical properties of the silicon through a number of different processes, including generation (thermal generation of e-h pairs), recombination (charge is captured and is effectively lost) and trapping (charge is captured and released after some period of time)[1]. The impact of these defects is subject to the energy level created within the silicon bandgap, related to the type of impurity forming the defect, the speed at which charge is moving and the temperature of the silicon. The susceptibility of the detector is dependent on the method used to readout the detector, a Charge-Coupled Device (CCD) requires a number of charge transfers compared to the one transfer typically required by a Complementary Metal-Oxide Semiconductor image sensor (CMOS). Making the radiation induced Charge Transfer Efficiency (CTE) of particular interest for operating a CCD in space, and it is the radiation induced degradation to CTI that is the focus of this paper.

The type of defect which will have the most impact on charge transfer within the CCD is linked to the type of material in which the charge transfer takes place, n-type silicon (phosphorous dopant) or p-type silicon (boron deponent). In n-channel CCDs the dominant traps pre-irradiation have energies of 0.12 eV and 0.30 eV below the conduction band, the former is the oxygen vacancy and the latter is believed to be vacancy related[2]. The concentration of these defects increases after irradiation and an additional trap is generated with an energy of around 0.42 eV below the conduction band which is attributed to the phosphorous vacancy (E-centre). It was first demonstrated that a p-channel CCD could offer increased tolerance to displacement damage in 1997[3], the improved tolerance has since been demonstrated in a number of other studies comparing p-channel and n-channel performance[4-8].

*jason.gow@open.ac.uk; phone +44 (0)1908 332194; www.open.ac.uk/cei

The dopant used in p-channel is boron; boron has not been shown to have the same impact on CTE as the phosphorous dopant used in n-channel devices. Therefore, immediately there is less concentration of impurities from which stable defects can be formed that could impact charge transfer. The radiation induced defects which increase Charge Transfer Inefficiency (CTI) in a p-channel CCD have been linked to the divacancy and other traps related to carbon and oxygen interstitials[4-8, 11-12]. As there are less radiation induced defects in a p-channel CCD which have been shown to increase CTI and because they are formed in smaller quantities (the divacancy is a second order defect and boron defects have not been shown to impact CTE) when compared to an n-channel equivalent, p-channel CCDs are more hard to radiation induced CTI.

When considering the number of traps that could form during the irradiation and the capture and emission time of holes, described by Shockley-Read-Hall theory[12-13], a p-channel CCD should provide more options for optimal timings to be selected. The measured CTI is closely linked to the emission time constant, τ_e, and it will be low if τ_e is very much less than the time allowed to re-join the charge packet (*i.e.* the trap is too fast to impact performance) or if τ_e is very much greater than the time between events of interest, in the case of this paper X-rays (*i.e.* a high probability that the trap will remain filled and unable to capture further charge of interest). To enable an optimal window of charge transfer to be selected the operational temperature and transfer times need to be considered, which raises the issue of defect mobility.

Typically a proton irradiation performed to investigate post-irradiation performance for a space mission is performed at room temperature, however, based on the evidence from other studies looking into the performance of devices irradiated at cryogenic temperatures[3,6-12,15-17], this may not provide the conditions to allow appropriate minimisation of radiation induced CTI. This is because of the mobility of individual defects after the irradiation and their ability to interact with other defects to form different defects. The resulting change in CTI and trap concentrations has been shown by the aforementioned studies to be related to the temperature of the silicon. Therefore, the defects that will impact charge transfer are related to the thermal history of the device during and after the irradiation. To ensure the optimal operating conditions can be selected the type and quantities of defects present need to be determined, the best way to achieve this is by irradiating the device using appropriate mission operating conditions, *i.e.* holding the device at mission operating temperature with the device powered and clocking.

The study described in this paper was performed as part of a European Space Agency (ESA) funded investigation (TEC-MME/2012/298) into the performance benefits provided through the use of a p-channel rather than an n-channel CCD[10-12]. The overall aim of the study was to build upon our understanding of device behaviour and the impact of performing irradiations at cryogenic temperatures and how the observed defect concentrations linked to CTI measurements. This paper focuses on the CTI measurements made using X-rays and the defects impacting charge transfer from a device irradiated at 153 K and the subsequent impact on these measurements after the device had been allowed up to room temperature for a period of 26 hours, during which time the device was un-biased. The data collected after the device had been held at room temperature for a further week, three weeks and eleven weeks will form part of a future publication.

1.1 CCD204

The e2v technologies CCD204, shown in Figure 1, is manufactured on high resistivity bulk n-type silicon thinned to 70 μm (fully depleted). It is a 4k × 1k device with 12 μm square pixels, utilising a split register with two output nodes each of which can be operated using an amplifier responsivity of 4.5 μV/h^+ or 1.5 μV/h^+. Both p-channel[8, 11-12] and n-channel[8, 18] variants of excellent quality have been produced.

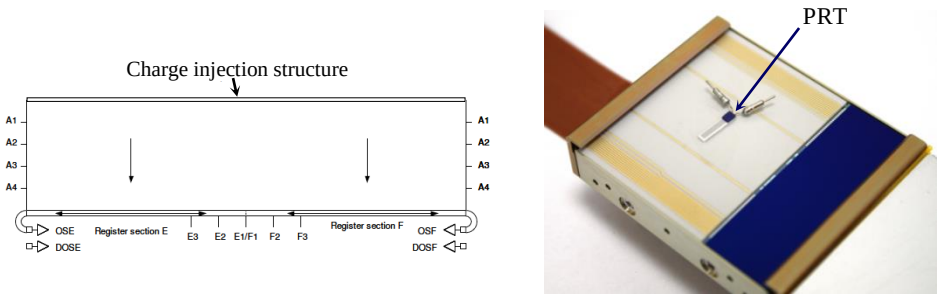

Figure 1. Schematic and photograph of the e2v technologies CCD204-22. The photograph shows the location of the platinum resistance thermometer (PRT) used to monitor the temperature of the device during data collection.

2. EXPERIMENTAL ARRANGEMENT

The irradiation was performed using 7.5 MeV protons from the Synergy Health 5MV Tandem accelerator (UK), with the device under test held in a modified Centre for Electronic Imaging (CEI) vacuum test facility, shown in Figure 2 mounted on the end of the proton beamline. The CCD under test was clamped onto a copper cold bench connected to a CryoTiger® refrigeration system with the temperature controlled using a feedback system, comprising a Lakeshore 325 temperature controller, platinum resistance thermometer (PRT), and a heater. An XTF5011/75-TH X-ray tube was used to fluoresce a polished manganese target held at 45° to the incident X-ray beam to provide around one X-ray event per eighty pixels. Clocking and biasing were provided by an XCAM Ltd. USB2REM2 camera drive box in conjunction with drive software controlled use a custom MatLab software program.

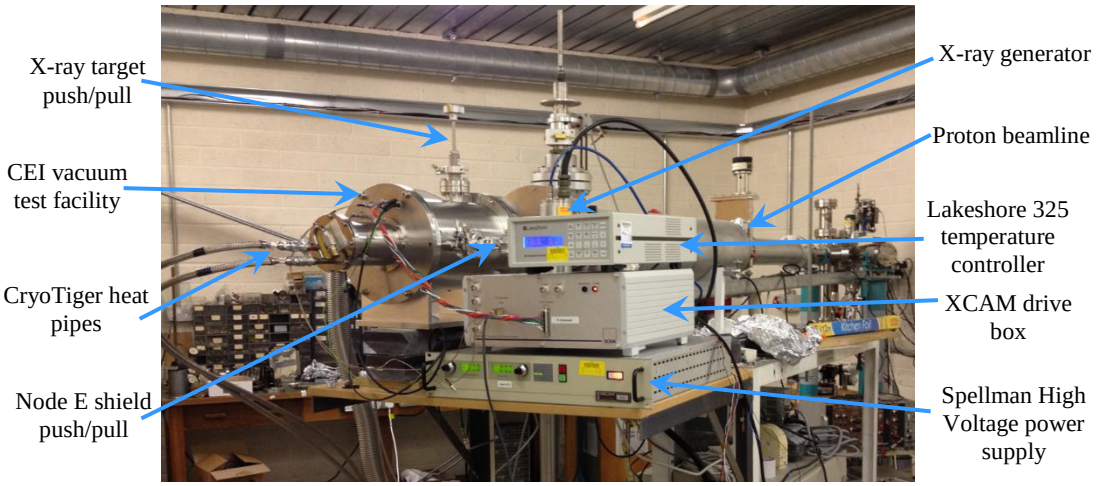

Figure 2. Photograph of the CEI vacuum chamber attached to the end of the Synergy Health proton beamline.

2.1 Proton Irradiation

The area irradiated on each device is shown in Figure 3. This region of irradiation was selected to provide an on-chip control, *i.e.* the region next to the output node was left un-irradiated, while still allowing an assessment of parallel and serial CTE to be performed. Details on the flux and 10 MeV equivalent fluence delivered to each device is given in Table 1, no change was observed to the control devices performance. The regions irradiated with a 10 MeV equivalent proton fluence of 1.24×10^{11} protons.cm^{-2} in the cryogenic device was not used to generate data for this paper because of the poor CTI making automated, and hence repeatable, CTI measurements difficult.

Device	Details	Image Region	7.5 MeV proton fluence (protons.cm^{-2})	7.5 MeV flux (protons.cm^{-2})	10 MeV equivalent proton fluence (protons.cm^{-2})
10092-04-03	Control	AE	Control Device		
		AF			
10092-06-02	Room Temp	AE	1.53×10^{9}	2.0×10^{7}	2.0×10^{9}
		AF	3.07×10^{9}	2.0×10^{7}	4.0×10^{9}
10092-04-05	Cryogenic	AE	9.50×10^{8}	2.5×10^{7}	1.24×10^{9}
		AF	9.50×10^{10}	2.5×10^{7}	1.24×10^{11}

Table 1. Proton irradiation details for the room temperature and cryogenic irradiation

During the irradiation the X-ray target was raised out of the beam using the push-pull labelled in Figure 2. The 10 mm thick aluminium proton shields were attached to rotational push pulls to enable to shields to be moved into and out of the beam, thereby allowing the two nodes to be irradiated with a different fluence. Data collection with the room temperature irradiated devices was performed at the Open University after the 26 hour anneal assessment of the cryogenic device had been completed.

During the cryogenic irradiation the CCD was held at 153 K, it was biased and acquiring images. Data collection at Harwell was performed with the gate valve closed to isolate the test chamber from the beamline, after both nodes had been irradiated the chamber was disconnected from the beamline to enable the CCD performance at 153 K to be monitored for 7 days after the irradiation, during this time the device was operating and collecting data. The same equipment was re-assembled at the Open University to allow data collection to be performed after the device was allowed back to room temperature. While at room temperature the device was un-biased.

3. EXPERIMENTAL TECHNIQUE

The CCD204 was readout at 200 kHz using a parallel transfer pulse time (t_{oi}) of 1,000 µs. To collect the thirty images used to measure the X-ray CTI an integration time of 10 s was used, with the X-ray tube automatically turned on at the start of the integration time and then turned off 0.3 s before the end of the integration period. This results in an X-ray density of 1 X-ray event per 80 pixels across the image. The readout speed and X-ray density were the same as used during data collection with an n-channel CCD204[18], however the integration time used in the n-channel CCD was 500 s this had to be reduced for p-channel operation due to time constraints on data collection. The n-channel data used to make the comparison was collected at 150 K.

The same analysis code was used to analyse both n-channel and p-channel data. The CTI analysis was performed by dividing the CCD into bins, 30 pixels wide, and the peak location identified by fitting a Gaussian to the Mn-Kα X-ray events within each successive bin. The CTI was then measured using the gradient of the line of best fit applied to the data and the X-ray signal $X(e^-)$, in the form[19]

$$CTI_X = \frac{S_D(e^-)}{X(e^-)n_t} \tag{1}$$

where $S_D(e^-)$ is the average deferred charge, and n_t is the number of pixels transfers. The error on the CTI is calculated using the error on the weighted mean of the peak location and the error on the gradient, found using a parallelogram of error. The error from the equipment is taken as ± 1 ADC channel. An example fit to the X-ray peak location is given in Figure 3, the resulting X-ray scatter plot is also included.

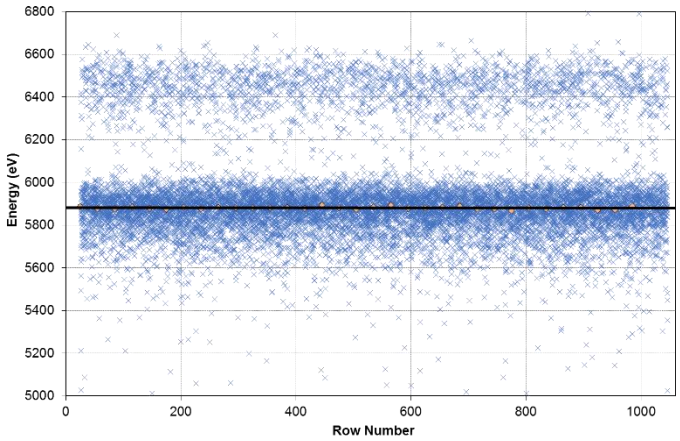

Figure 3: X-ray scatter plot measured at 188 K using node F of device #10092-04-03, the peak locations and resulting linear fit used to calculated the parallel CTI are also included

A total of 30 images were collected using the p-channel CCD204 for each variable explored, example X-ray scatter plots for parallel transfers are shown in figures 4 and 5 for pre-irradiation and after the CCD had been irradiated with a 10 MeV equivalent fluence of 1.24×10^{9} protons.cm^{-2} at 153 K. The impact of the additional traps formed as a result of the incident radiation is clear by the increase in the gradient of the line of best fit. The increase in the spread in the X-ray data shown in Figure 5 is as a result of the charge transfer within an irradiated serial register. To enable a comparison of data between the cryogenically irradiated device and the p-channel and n-channel CCD204s irradiated at room temperature a linear fit to the data taken at the two different fluences shown in Table 1 was used to scale the results to a 10 MeV equivalent fluence of 1.24×10^{9} protons.cm^{-2}.

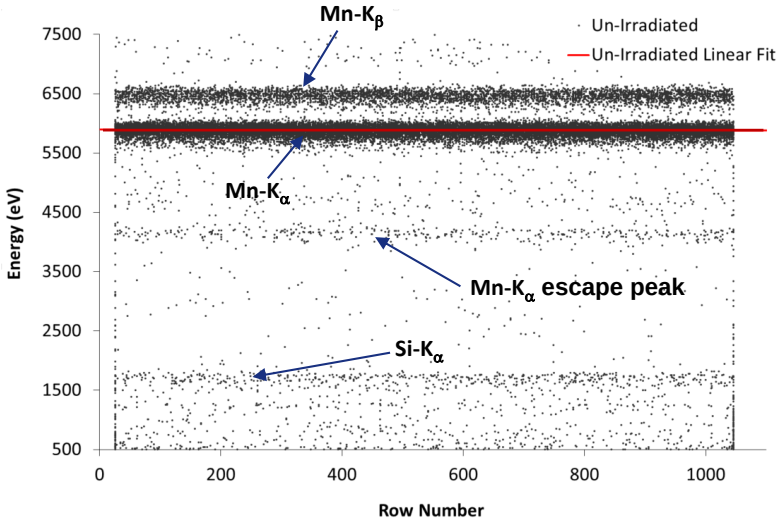

Figure 4: X-ray scatter plot measured at 153 K using node F of device #10092-04-05 pre-irradiation, the resulting linear fit used to calculated the parallel CTI is also included

The trap pumping analysis relies on moving the charge backwards and forwards in the parallel direction. The intensity of the resulting dipole is dependent on the phase time, t_{ph}, increasing to the point at which the trap has maximum effect is most efficient and then decreasing as the t_{ph} is increased further. The emission time constant of the trap can then be calculated by fitting[20]

$$Dipole\ Amplitude = NP_C\left(exp\left(\frac{-t_{ph}}{\tau_e}\right) - exp\left(\frac{-2t_{ph}}{\tau_e}\right)\right) \quad (2)$$

where N is the number of pumping cycles (in this study 4,000), P_C is the probability of capture and τ_e is the emission time constant. The t_{ph} was be varied from 7 µs to 30,500 µs for a complete trap sweep to produce a dipole intensity curve.

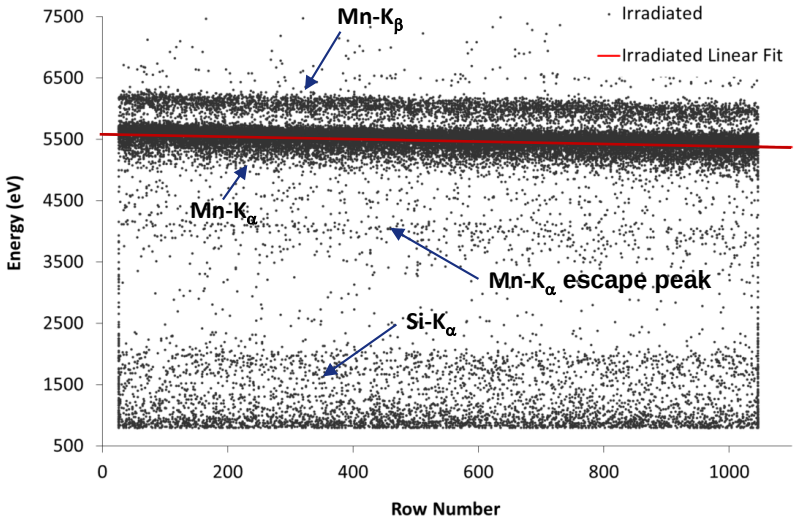

Figure 5: X-ray scatter plot measured at 153 K using node F of device #10092-04-05 around 100 hours after the device has been irradiated at 153 K, the resulting linear fit used to calculated the parallel CTI is also included

4. RESULTS AND DISCUSSIONS

The CTI measured in the control region of the CCD irradiated at room temperature and at 153 K was within error for all variables examined both pre- and post-irradiation. The number of defects identified in a region of 239k pixels as a function of time after the irradiation is shown in Figure 6, there is a clear increase, around 820%, in the number of defects classified as the divacancy after the device had been allowed up to room temperature for 26 hours and a smaller reduction, around 55%, in the number of defects identified as the carbon interstitial after the device had been allowed up to room temperature for 26 hours. This data was collected to enable observed changes in CTI performance to be linked to the defects present within the device at that time and also to enable an investigation into the defect evolution to be performed.

The X-ray CTI in the parallel direction demonstrated a clear increase post irradiation at 153 K, shown in Figure 7, after irradiation with 1.24×10^9 protons.cm^{-2}. This was followed by a decrease in the value outputted from the analysis after the device had been allowed to rest at room temperature for 26 hours, followed by two small increases after the one and three additional weeks rest at room temperature. The time between successive X-ray events, around 1.5 s, is considerably longer than the τ_e of the two traps identified and considerably smaller than the τ_e of the C_iO_i defect reported by Mostek *et al.*[9]. Therefore this should have a negligible impact on the observed CTI. The C_iO_i defect is too slow at 153 K to have been detected by the range of t_{ph} value used during this study, a future publication will explore the trap pumping and CTI measurements made over a range of temperatures. The time in which the charge can re-join the charge packet is primarily linked to the t_{oi}, the value of 1,000 µs was selected to provide optimal transfer based on an optimisation of a room temperature irradiated CCD204 to provide a factor of around 100 difference between the t_{oi} and the divacancy τ_e[8], giving only a factor of 10 between the t_{oi} and the C_i τ_e. The parallel dwell time, the time required to perform one serial transfer, is comparable to the emission time constant of the C_i defect and this too will mean that the C_i defect should impact parallel charge transfer more than the divacancy.

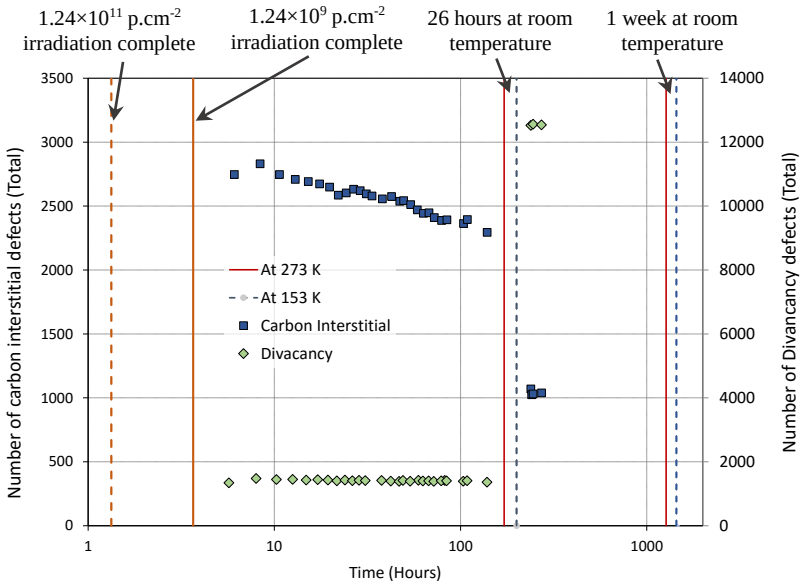

Figure 6: Number of traps identified as carbon interstitials and divacancies as a function of time after the irradiation and the first 26 hours the device was held at room temperature[11-12]

Therefore considering the observed changes in trap concentrations shown in Figure 6 the reduction in parallel CTI after the 26 hours at room temperature could be linked to the reduction in C_i defects with a small negative impact as a result of the considerable increase in divacancy defects. It could be possible, for a device that will be irradiated at 153 K and not allowed up to room temperature, to operate with a lower t_{oi} for improved CTI. This is because the number of divacancies is low when compared to the number of C_i defects after the irradiation. The advantage of a lower t_{oi} for device operation is an increased frame rate.

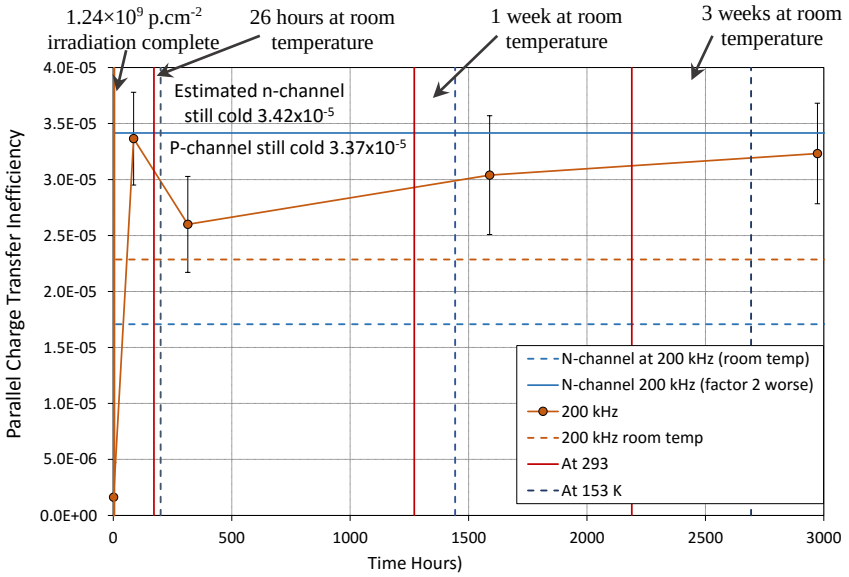

Figure 7: Parallel X-ray CTI measured at 153 K using the device irradiated at 153 K, pre- and post-irradiation and after three different time periods with the device held un-biased at room temperature

The X-ray CTI in the serial direction demonstrated an increase post irradiation at 153 K, shown in Figure 8, a factor of 2 less increase when compared to the parallel direction. This was followed by a significantly larger increase after the device had been allowed to rest at room temperature for 26 hours, followed by a small decrease after one additional week rest at room temperature and a slight increase after a further three weeks. These changes are negligible when compared to the measured values. The time between successive X-ray events, around 4.0×10^{-4} s, is around a factor 10 greater than the divacancy τ_e and around a factor 200 smaller than the C_i τ_e at 153 K based on the values reported by Mostek *et al.*[9]. The time to re-join of 1.7×10^{-4} s a factor of 10 smaller than the divacancy τ_e and considerably smaller than the C_i τ_e at 153 K. Therefore the divancancy defect should have a considerably greater impact on the serial CTI compared to other p-channel defects.

Therefore considering the observed changes in trap concentrations shown in Figure 6, the increase post irradiation is primarily the result of the increase in the divacancy, and the 470 % increase after the room temperature anneal can be linked to the significant increase in the number of divacancy defects. This suggests that, should the temperature remain at 153 K post irradiation, it would be possible to operate the CCD faster with only a small loss in serial CTI, further increasing the frame rate which could be achieved. It is interesting to note that the increase in CTI does not correspond directly to the 820% increase in defects identified as divacancies, this is because the relationship between charge transfer and τ_e is not as simple as comparing one time value and requires a more in-depth approach to optimisation, to be discussed in a subsequent publication.

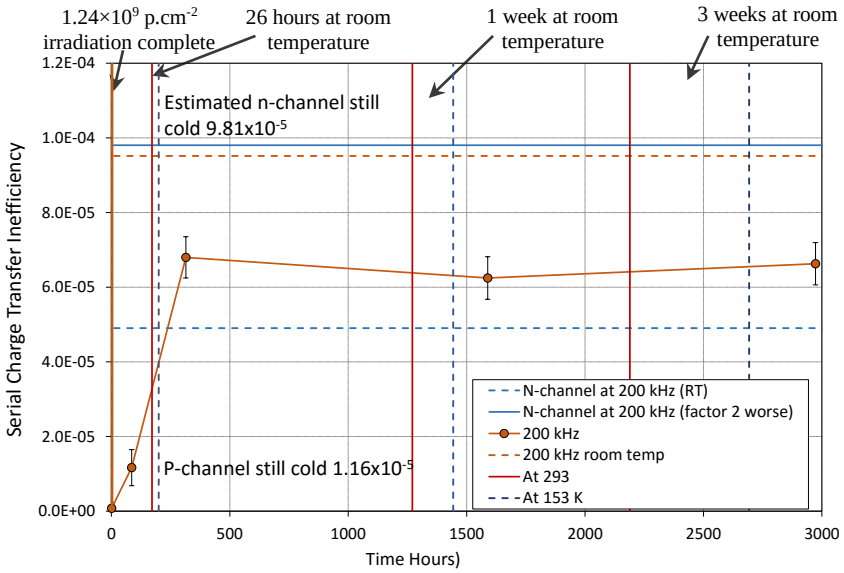

Figure 8: Serial X-ray CTI measured at 153 K using the device irradiated at 153 K, pre- and post-irradiation and after three different time periods with the device held un-biased at room temperature

The estimation of the CTI in the p-channel device irradiated at room temperature, assuming a linear increase in CTI with fluence, to a 10 MeV equivalent fluence of 1.24×10^9 protons.cm^{-2} does not compare well to the measured values from the cryogenic device after time spent at room temperature. The parallel CTI is slightly higher (considering the error on the measurements the results are similar) and serial CTI is a factor of 1.4 lower, as shown in Figure 7 and 8 respectively. The differences are likely linked to the mobility of the defects as the device was allowed up to room temperature and the types of stable defects which are formed. Thereby resulting in different defect concentrations when compared to the device which was irradiated at room temperature, the performance of the cryogenically irradiated device will continue to be monitored periodically.

To enable a comparison to data collected with an n-channel CCD204 irradiated at room temperature[18] the estimated performance after a 10 MeV equivalent fluence of 1.24×10^9 protons.cm^{-2} based on a linear fit to data collected at 150 K was scaled using a factor of 2^{17}, to estimate cryogenic performance. The estimated room temperature and cryogenic performance of the n-channel CCD is included in figures 7 and 8 for parallel and serial CTI respectively. In the case of

parallel transfers the performance appears to be comparable, it is in the serial direction where the p-channel CCD indicates a factor of around 8.5 improvement over the estimation of n-channel performance.

5. CONCLUSIONS

The reported behaviour in CTI measured post-irradiation at 153 K and again at 153 K after the device had been allowed to rest at room temperature for different periods of time, un-biased, are dynamic, particularly in the case of the serial transfer at 200 kHz. The behaviour has been linked to the observed changes in trap population of defects identified as the divacancy and carbon interstial. In particular the large increase in serial CTI after the device had been allowed up to room temperature for 26 hours has been linked to the large increase in the number of divacancy defects. The increase in serial CTI is not the same factor of increase observed in the number of divacancy defects, this is because the relationship between charge transfer and τ_e is not as simple as comparing one time value and requires a more in-depth approach to optimisation, to be discussed in a subsequent publication.

The difference in performance in the cryogenically irradiated CCD after irradiation and its performance after it had been allowed to rest at room temperature and the performance of the CCD irradiated at room temperature, clearly indicate that if you want to provide the best estimate of inflight performance you need to irradiate the device at a mission appropriate temperature. This will also enable an effective optimisation to be performed to select the optimal clock timings and temperature to mitigate against radiation induced CTI[23].

The comparison to the n-channel CCD204 estimated performance under cryogenic irradiation conditions indicates similar performance for parallel transfers but a factor of around 8.5 improvement for serial transfers. It should be noted that this comparison relies on a number of assumptions, a true comparison should ideally compare the performance of both devices when operated using optimal conditions. A study is proposed to investigate this using a p-channel CCD204 and n-channel CCD204 irradiated side by side at the same time and operated at the same time using the same drive electronics.. The study will look into the defect formation and evolution within the two types of CCD204[21] and the CTI[22] after the devices have been irradiated under cryogenic conditions at 153 K and 203 K.

ACKNOWLEDGMENTS

The authors would like to thank Keith Jones of Synergy Health for his assistance during the proton irradiation, and Ludovic Duvet, Thibaut Prodhomme, Alessandra Ciapponi and Yves Levillain of ESA for their support during this study.

REFERENCES

[1] Srour, J. R., Marshall C.J., and Marshall P.W., “Review of Displacement Damage Effects in Silicon Devices,” IEEE Trans. Nucl. Sci. 50(3), (2003).

[2] Holland, A. D., “The effect of bulk traps in proton irradiated EEV CCDs,” Nuclear Instr. Meth. Physics Res A326, 335–343 (1993).

[3] Spratt, J. P., Passenheim, B. C. and Leadon, R. E., “The Effects of Nuclear Radiation on P-channel CCD Imagers,” IEEE Radiation Effects Data Workshop, 116-121 (1997).

[4] Hopkinson, G. R., “Proton damage effect on P-channel CCDs,” IEEE Trans. Nucl. Sci., 46(6), 1790-1796 (1999).

[5] Bebek, C., Groom, D., Holland, S., et. al., “Proton Radiation Damage in P-channel CCDs Fabricated on High-Resistivity Silicon,” IEEE Trans. Nucl. Sci., 49(3), 1221-1225 (2002).

[6] Spratt, J. P. et al., “Proton Damage Effects in High Performance P-Channel CCDs,” IEEE Trans. Nucl. Sci., 52(6), 2695-2702 (2005).

[7] Dawson, K., Bebek, C., Emes, J., et al., “Radiation Tolerance of Fully-Depleted P-Channel CCDs Designed for the SNAP Satellite,” IEEE Trans. Nucl. Sci., 55(3), (2008).

[8] Gow, J. P. D., Murray, N. J., Holland, A. D., and Burt, D., “Proton damage comparison of an e2v technologies n-channel and p-channel CCD204,” IEEE Trans. Nucl. Sci., 61(4), 1843–1848 (2014).

[9] Mostek, N. J., Bebek, C., Karcher, A., et al., “Charge trap identification for proton-irradiated p+ channel CCDs,” Proc. SPIE 7742, (2010).

[10] Murray, N. J., Holland, A. D., Gow, J. P. D., et al., “Assessment of the performance and radiation damage effects under cryogenic temperatures of a P-channel CCD204s,” Proc. SPIE 9154, (2014).

[11] Gow, J. P. D., Wood, D., Burt, D., Hall, D. J., Dryer, B., Holland, A. D. and Murray N. J., “Initial Results from a Cryogenic Proton Irradiation of a p-channel CCD,” Proc. SPIE 9601, (2015).

[12] Gow, J. P. D., Wood, D., Murray, N. J., Burt, D., Hall, D. J., Dryer, B., Holland, A. D., "Postirradiation behavior of p-channel charge-coupled device irradiated at 153 K," J. Astron. Telesc. Instrum. Syst. 2(2), 026001, (2016).

[13] Shockley, W., and W. Read, T. Jr., “Statistics of the Recombination’s of Holes and Electrons,” Physical Review 87(5), 835-842 (1952).

[14] Hall, R. N., “Electron-Hole Recombination in Germanium,” Physical Review 87(5), 387-387 (1952).

[15] Bautz, M., Prigozhin, G., Kissel, S., et al., “Anomalous Annealing of a High-Resistivity CCD Irradiated at Low Temperature,” IEEE Trans. Nucl. Sci. 52(2), (2005).

[16] Grant, C. E., LaMarr, B., Prigozhin, G. Y., et al., “Physics of reverse annealing in high-resistivity Chandra ACIS CCDs,” Proc. SPIE 7021, (2008).

[17] Hopkinson, G.., Short, A., Vetel, C., et al., “Radiation Effects on Astrometric CCDs at Low Operating Temperatures,” IEEE Trans. Nucl. Sci. 52(6), 2664-2671 (2005).

[18] Gow, J. P. D., Murray, N. J., Holland, A. D., et al., “Assessment of space proton radiation-induced charge transfer inefficiency in the CCD204 for the Euclid space observatory,” JINST, 7 C01030, (2012).

[19] Janesick, J. R., [Scientific Charge Coupled Devices], SPIE Press Washington, (2001).

[20] Hall, D. J., Murray, N. J., Holland, A. D., et al., “Determination of in situ trap properties in CCDs using a single-trap pumping technique,” IEEE Trans. Nucl. Sci. 61(4), 1826–1833 (2014).

[21] Gow, J. P. D., and Murray, N. J., “P-Channel CCD Performance Characterisation and Radiation Testing: P-channel and N-channel Comparison Test Proposal,” OU-PCHAN-TN-08, (2016).

[22] Gow, J. P. D., “CCD versus CIS in the Context of Harsh Radiation Environment Missions: Test Plan,” OU-CCDvCIS-TN-03, (2016).

[23] Murray, N. J., *et al.*, “Mitigating radiation-induced charge transfer inefficiency in full-frame CCD applications by 'pumping' traps,” Proc. of SPIE 845317, (2012).